Structural Effect of La Modified PbTiO$_3$ Perovskites

N SAHU[1*] and M KAR[2]

[1]P.G. Department of Physics, G.M. University, Sambalpur-768004, Odisha, India.
[2]Department of Physics, Indian Institute of Technology Patna, Patna 800013, Bihar, India
E-mail: nsahu76@gmail.com

Abstract. The Pb$_{1-x}$La$_x$TiO$_3$ (for x=0.0, 0.10, 0.25, 0.30 and 0.50) compounds were prepared by conventional solid state route. The X-ray diffraction (XRD) pattern was recorded at room temperature and the samples were found in single phase form. The pure samples (x=0) could be indexed to *P4mm* space group in tetragonal symmetry, but the doped samples could be indexed using $Pm\bar{3}m$ space group in cubic symmetry. XRD pattern has been analyzed by employing Rietveld method with the help of FullProf Program. The bond lengths and angles have been calculated by using Powder Cell Programme. We have observed that, the Pb-Ti, Ti-O$_1$, Ti-O$_2$, Pb-O$_1$ and Pb-O$_2$ bond lengths decreased with the increase in La concentration and also Ti-O$_1$, and Pb-O$_2$ distances are statistically different from pure and doped samples due to its structural changes and symmetry dependence. The crystallite size was obtained by using Scherrer method, Hall-Williamson method, and Rietveld refinement method. It is observed that crystallite size decreases with increase La concentration for both the annealed samples.

Keywords: Ceramic; Rietveld; FullProf; XRD; Crystallite size.

PACS NO: 77.80.–e, 75.40.Cx,

1. Introduction

The mineral perovskite is CaTiO$_3$ and is actually orthorhombic at room temperature, becoming cubic at temperatures above 900°C [1]. Lead titanate (PbTiO$_3$), which exhibits Perovskites structure and a very high Curie temperature T$_c$ = 490°C, belongs to the most important ferroelectric and piezoelectric families [2]. The perovskite structure has been one of the most versatile structures for tailoring the properties of materials [3, 4]. The Pb-based ceramic oxides have been widely studied due to their excellent ferroelectric, dielectric, and piezoelectric properties [1–3]. Inparticular,PbTiO$_3$-based solid solutions have dominated for decades the technological field responsible for the development of

piezoelectric materials [4]. The perovskite structure forms the basis of several complex structures, which may be due to intergrowths, oxygen deficiency or due to cation ordering [4, 5]. It has been shown that modification using aluminium, which occupies the B-sites, provides new structural defects, i.e. oxygen vacancies, during the sintering process [6]. Lead oxide also forms a liquid phase above its melting point (890°C), which improves densification, but it also may affect the stoichiometry of the composition, due to its high volatility at the sintering temperatures. Therefore, an excess PbO is usually added to the initial raw materials, in order to prevent the deviation from the stoichiometry by lead loss and also to improve the densification. Lead titanate $PbTiO_3$ (PT) and lead lanthanum titanate $Pb_{1-x}La_xTiO_3$ (PLT) are important perovskite ferroelectric materials which show remarkable ferroelectricity, piezoelectricity and pyroelectricity, because of their potential applications in the field of microelectronics and optoelectronics. Lead titanate ($PbTiO_3$) has the perovskite (ABO_3) structure with the Pb atoms occupying the cell corners, Ti occupying the body canter, and the oxygen atoms sitting at the face centers[7,8]. The isomorphic substitution of lead with lanthanum gives rise to a decrease in the tetragonality [9]. The PT undergoes a phase transition at a temperature of 490˚C from tetragonal (*P4mm*) ferroelectric phase to centrosymmetric cubic ($Pm\bar{3}m$) paraelectric phase [10-13]. An appropriate incorporation of La into lead titanate tunes the phase transition temperature and consequently makes the PLT material suitable for a wide range of device applications at room temperature. R. D. S*hannon,* [14] reported that in La^{3+}modified $PbTiO_3$ materials, La^{3+} replaces Pb^{2+} rather than Ti^{4+} in Pb-based perovskites. To keep the neutrality of the charge, since that replacement is aliovalent, site vacancies are created. *E. C. S. Tavares, et al* [15] observed that in La modified PT ceramics for temperatures higher than Tc, a residual short-range structural disorder has been found, which is not to be compatible with the centrosymmetric cubic structure usually observed in the paraelectric phase. It has been suggested that the lanthanum-induced modification concerning $PbTiO_3$ results in structural changes that can be directly related to the nature of the phase transition [16-20].

2. Experimental Technique

The $Pb_{1-x}La_xTiO_3$ (for x=0.0, 0.10, 0.25, 0.30 and 0.50) compounds were prepared by conventional solid state route. The stochiometric ratio of starting compounds such as Lead Oxide (PbO, 99%), Lanthanum Oxide (La_2O_3, 99.9%) and Titanium Oxide (TiO_2, 99%) were weighed by using a high precision electronic balance. The above compounds were mixed and grinded under acetone

using agate mortar and pestle. The grinding was carried out under acetone till the acetone evaporates from the mortar. The mixture was ball milled for 8 h for homogeneous mixture and calcined at $900^{o}C$ for 6h and for phase conformation XRD was taken. The fine powders of the above compound were pressed into cylindrical pellets of 6 mm diameter and 1 mm thickness under a uni-axial pressure of 6 ton using a hydraulic press. Finally the pellets were sintered at $1100^{o}C$ for over 4h with 5% extra lead oxide to compensate the lead loss at high temperature and then cooled to room temperature at the rate of $2^{o}C$ min^{-1}. All the above sintering processes were carried out in the air. The XRD patterns of all the samples were recorded by using Philips PANalytical X'pert-MPD X-ray diffractometer (XRD) (Model- PW3020) in the department of ceramic engineering, NIT, Rourkela. The CuKα radiation was used as an X-ray source. The machine was operated at 35KV and 30mA. The data were collected with step size of 0.020 and time constant of 1 second. The various steps in the solid-state reaction process are represented as a flow chart shown in Fig.1.
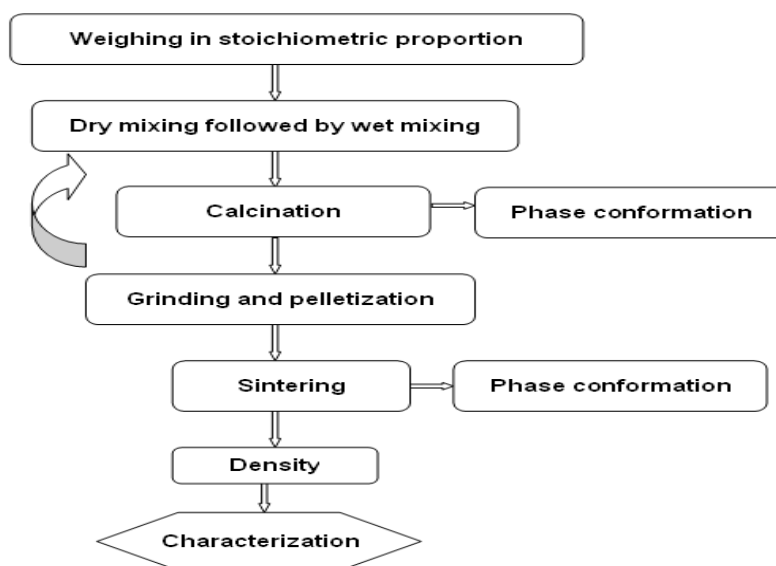

Fig. 1: Flow chart describing the various steps involved in solid-state reaction route.

3. Results and discussion

The X-ray diffraction (XRD) patterns were recorded in all the samples at room temperature. The XRD patterns of $Pb_{1-x}La_xTiO_3$ (PLT) for x = 0, 0.10, 0.25, 0.30 and 0.50 calcined at $900^{0}C$ for 6 h. (Fig. not given here). The single phase

XRD patterns of pure sample for x = 0 could be indexed to *P4mm* space group in tetragonal symmetry. However, the doped samples for x = 0.10, 0.25, 0.30 and 0.50 could be indexed using $Pm\bar{3}m$ space group in cubic symmetry. The overlap of the three tetragonal reflections (102), (201) and (210), confirms the tetragonal-to-cubic phase transition. We have not observed any peak corresponds to *P4mm* space group in the XRD pattern of x = 0.10 samples. In PLT10, these reflections coalesce according to the cubic multiplicity of (210). Hence, it has been found that a phase transition from tetragonal to cubic symmetry with increase of La concentration. However, *P.P.Neves et al* [1] has been reported that, the phase transition occurs at x ~0.25 on $Pb_{1-x}La_xTiO_3$ material. The XRD patterns of $Pb_{1-x}La_xTiO_3$ (PLT) compound for x = 0, 0.10, 0.25, 0.30 and 0.50 sintered at 1100˚C for 4h respectively is shown in fig,2. We have not observed any additional peak in 1100^0C sintered samples compare to that of 900^0C calcined sample. It reveals that, the structure does not change with the increasing of annealing temperature. However the crystallite size increases with the increasing of sintering temperature. In the pure sample ($PbTiO_3$), the Ti, O_1 and O_2 are positively shifted along c direction, whereas in the doped sample, structure $Pm\bar{3}m$, these atoms occupy exactly the corners (A site), the face centers (oxygen's sites), and the body center (B site) of the unit cell, which means the ideal perovskite cubic structure.
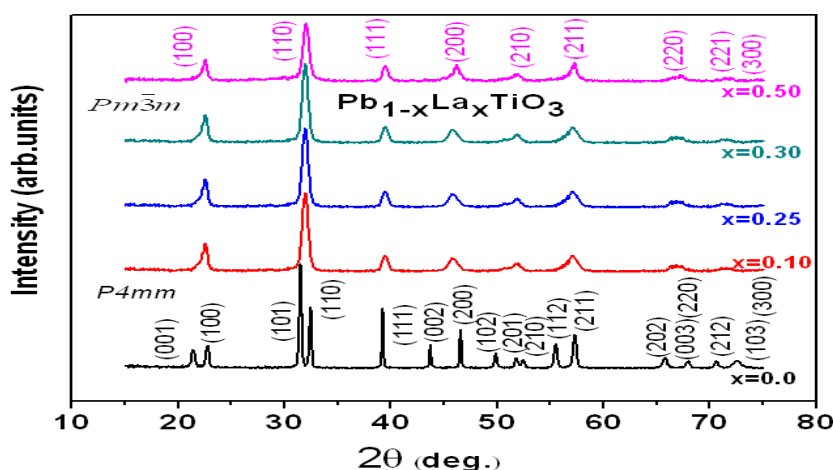

Fig.2: XRD patterns of $Pb_{1-x}La_xTiO_3$ (PLT) compound for x = 0, 0.10, 0.25, 0.30 and 0.50 sintered at 1100˚C for 4h respectively.

The XRD pattern of pure and a typical doped sample PLT10 sintered at 1100˚C for 4h with refined data obtained by Rietveld method is shown in fig.3. and fig.4 respectively. The experimental points are given as plus (+) and

theoretical data are shown as solid lines. The difference between theoretical and experimental data is shown as a bottom line. The vertical and lines represent the Bragg's allowed peaks. For all La-containing $PbTiO_3$ samples, the A-site occupancy was shared between Pb and La. Considering A-site vacancies only, the refinements of the sample containing unrealistic values for the atomic occupancies and worse statistical compatible parameters, even for the samples with high La content. Nevertheless, it is important to emphasize that realistic occupancy results depend on the atomic number difference between the atoms involved in the site occupancy refinements. In this case, the Pb (82) and La (57) atomic numbers are significantly different, which usually permits a suitable occupancy refinement.
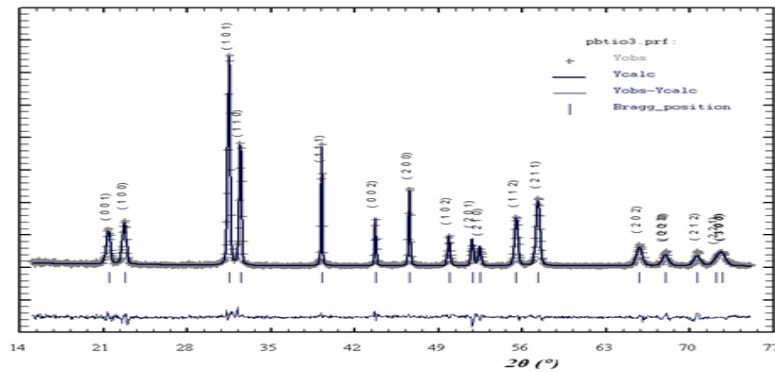

Fig. 3: XRD pattern of $PbTiO_3$ sintered at 1100˚C for 4h with refined data obtained by Rietveld method.
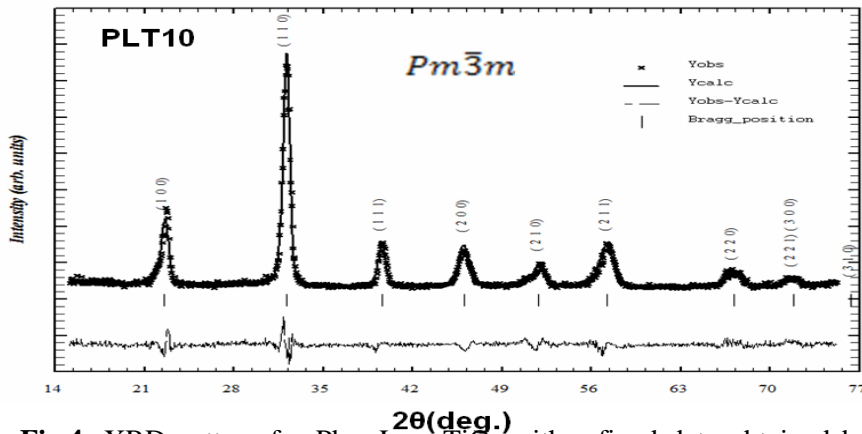

Fig.4: XRD pattern for $Pb_{0.90}La_{0.10}TiO_3$ with refined data obtained by Rietveld method.

The Lattice parameters, occupancy, fractional atomic positions etc. were taken as the free parameters during the fitting. The lattice parameters and unit cell volume was found to be decreased with the La concentration, it could be due to the smaller ionic size of La^{3+}(1.06 Å) compare to that of Pb^{2+}(1.20 Å). The Fractional atomic positions and isothermal parameter of the 1100^0C sintered sample $PbTiO_3$ and $Pb_{0.90}La_{0.10}TiO_3$ (PLT10) are shown in Table 1 and Table 2 respectively. The A-site occupancy, lattice parameters, cell volume, the goodness of the fitting parameter is listed in Table 3 for sintered samples only. The bond lengths and bond angles have been calculated by using a powder cell program. Also we have observed that, the Pb-Ti, Ti-O_1, Ti-O_2, Pb-O_1 and Pb-O_2 bond lengths decreased with the increase in La concentration. In fig.5 (a,b) , the variation of the Ti-O and Pb-O distances with lanthanum content for both calcined and sintered samples is presented. It can be observed that Ti-O_2 and Pb-O_1 separations remain nearly constant value throughout the whole series. This behavior was expected since Ti-O_2 and Pb-O_1 lie on the perpendicular plane to the ferro-distortive axis, which is unaffected by the c-axis distortion. On the other hand, it is observed that increasing La content, Ti-O_1, and Pb-O_2 distances are statistically different from pure and doped samples due to its structural changes and symmetry dependence. The values of bond lengths and angles are capitalized for sintered samples only in Table 3.

Table 1: Fractional atomic positions and isothermal parameter of the sample $PbTiO_3$ sintered at 1100˚C for 4h.

Atom	X	Y	Z	B_{iso}
Pb	0.00000	0.00000	0.00000	0.992 (2)
Ti	0.50000	0.50000	0.53770(6)	0.984(2)
O_1	0.50000	0.50000	0.11180(8)	1.000(3)
O_2	0.00000	0.50000	0.61740(5)	0.971(2)

Table 2: Fractional atomic positions and isothermal parameter of the sample $Pb_{0.90}La_{0.10}TiO_3$ sintered at 1100˚C for 4h.

Atom	X	Y	Z	B_{iso}
Pb	0.00000	0.00000	0.00000	0.992 (2)
La	0.00000	0.00000	0.00000	0.992 (2)
Ti	0.50000	0.50000	0.50000	0.984(2)
O_1	0.50000	0.50000	0.00000	1.000(3)
O_2	0.00000	0.50000	0.50000	0.97(2)

Table 3: Parameters obtained from Rietveld analysis of $Pb_{1-x}La_xTiO_3$ (PLT) powders for x = 0, 0.10, 0.20, 0.25 and 0.50 sintered at 1100ºC for 4 h respectively.

| Sample / Parameter	x=0.0	0.10	0.25	0.30	0.50
Space group	P4mm	$Pm\bar{3}m$	$Pm\bar{3}m$	$Pm\bar{3}m$	$Pm\bar{3}m$
Pb(Occup.)	0.9835(7)	0.8874(12)	0.7315(11)	0.6878(10)	0.4981(12)
La(Occup.)	0.00000	0.1095(11)	0.2324(10)	0.30404(4)	0.50842(7)
Ti(Occup.)	0.97200(2)	0.97200(2)	0.97200(2)	0.97200(2)	0.97200(2)
a = b (Å)	3.9491(3)	3.9402(8)	3.9385(11)	3.9343(14)	3.9321(5)
c (Å)	4.1304(9)	3.9402(8)	3.9385(11)	3.9343(14)	3.9321(5)
Volume (Å^3)	63.215(14)	63.151(4)	60.881(13)	60.472(7)	60.287(4)
χ^2 (chi^2)	2.04(4)	4.53(1)	4.53(1)	3.62(2)	2.37(7)
R_p	18.7(5)	22.1(7)	22.1(4)	21.4(7)	18.4(4)
R_{wp}	24.8(3)	28.8(7)	20.6(14)	27.6(17)	24.1(31)
R_{exp}	12.2(2)	12.4(6)	10.41(4)	12.1(10)	15.6(5)
R_{Bragg}	13.30(3)	12.49(1)	11.47(3)	12.71(3)	12.41(4)
R_f	8.28(20)	10.11(14)	5.10(21)	9.07(18)	7.74(22)
Pb-Ti (Å)	3.55(14)	3.47(11)	3.45(11)	3.41(14)	3.39(2)
Ti-O$_1$ (Å)	2.55(7)	2.53(3)	2.51(9)	2.48(6)	2.45(7)
Ti-O$_2$ (Å)	2.18(5)	2.17(6)	2.15(7)	2.14(9)	2.12(5)
Pb-O$_1$ (Å)	3.41(5)	3.40(2)	3.38(8)	3.36(8)	3.34(3)
Pb-O$_2$ (Å)	4.58(3)	4.47(7)	4.43(6)	3.96(4)	3.85(7)
∠Pb-Ti-O$_1$	71.96	102.13	102.73	102.73	102.73
∠Pb-Ti-O$_2$	84.01	145.5	145.5	145.5	145.5
∠Pb-Ti-Pb	77.19	71.52	71.52	71.52	71.52
∠O$_2$-Ti-O$_2$	107.14	149	149	149	149
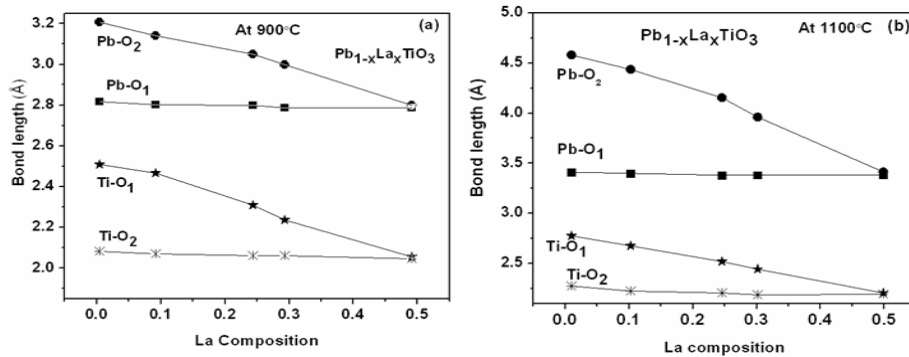
Fig.5 (a, b): The dependence of the Ti-O and Pb-O bond lengths with the La content of $Pb_{1-x}La_xTiO_3$ samples of x = 0, 0.10, 0.25, 0.30 and 0.50 (a) calcined at 900ºC for 6 h and (b) sintered at 1100˚C for 4h respectively.

X-ray diffraction is a simpler and easier approach for the determination of crystallite size of powder samples. The underlying principle for such a determination involves precise quantification of the broadening of the diffraction peaks. Based on this principle, a few techniques involving to calculate the crystallite size such as Scherrer method[21], Hall-Williamson method[22] and Rietveld refinement method [23]. The Crystallite size obtained from above three different methods is listed in Table 4. The crystallite size increases with increase of sintering temperature for both pure and substituted samples. The average crystallite size (obtained from above three methods) versus La concentration of $Pb_{1-x}La_xTiO_3$, x = 0.0, 0.10, 0.25, 0.30 and 0.50 samples is shown Fig.6 (a,b) (calcined at 900˚C and sintered at 1100˚C) respectively. Using the refined parameters the suggested stable crystal structure of $PbTiO_3$ and $Pb_{0.90}La_{0.10}TiO_3$ are shown in Fig.7. and Fig.8 (a-c) respectively.

Table 4: Average crystallite size (nm) calculated by various methods for the samples $Pb_{1-x}La_xTiO_3$ of x = 0.0, 0.10, 0.25, 0.30 and 0.50 calcined at 900˚C for 6h and sintered at 1100˚C for 4h respectively.

| Sample Composition	Crystallite size (nm)		
	Scherrer's Method	W.H. Method	Rietveld Method
$PbTiO_3$ (900˚C)	21.9(5)	18.7(11)	17.2(8)
$PbTiO_3$ (1100˚C)	44.2(5)	44.0(3)	43.2(2)
$Pb_{0.90}La_{0.10}TiO_3$ (900˚C)	19.8(3)	16.7(3)	15.3(11)
$Pb_{0.90}La_{0.10}TiO_3$ (1100˚C)	40.6(12)	40.1(11)	39.1(8)
$Pb_{0.75}La_{0.25}TiO_3$ (900˚C)	19.1(10)	15.1(4)	13.4(8)
$Pb_{0.75}La_{0.25}TiO_3$ (1100˚C)	38.5(7)	37.8(7)	36.1(2)
$Pb_{0.70}La_{0.30}TiO_3$ (900˚C)	17.8(6)	13.8(3)	12.2(9)
$Pb_{0.70}La_{0.30}TiO_3$ (1100˚C)	36.6(17)	35.3(13)	34.7(3)
$Pb_{0.50}La_{0.50}TiO_3$ (900˚C)	15.4(3)	12.4(5)	11.2(8)
$Pb_{0.50}La_{0.50}TiO_3$ (1100˚C)	34.0(4)	30.3(9)	29.3(5)
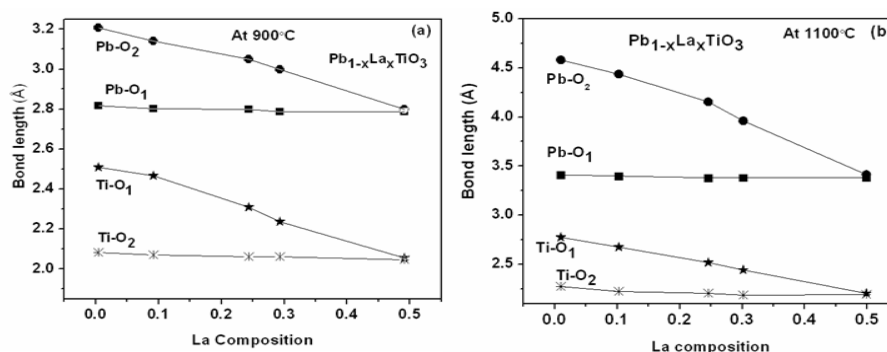
Fig.6.(a, b): The average crystallite size versus La concentration (a) calcined at 900˚C for 6h and (b) sintered at 1100˚C for 4h of $Pb_{1-x}La_xTiO_3$ (PLT) powders with (x=0, 0.10,0.25,0.30 and 0.50) respectively.
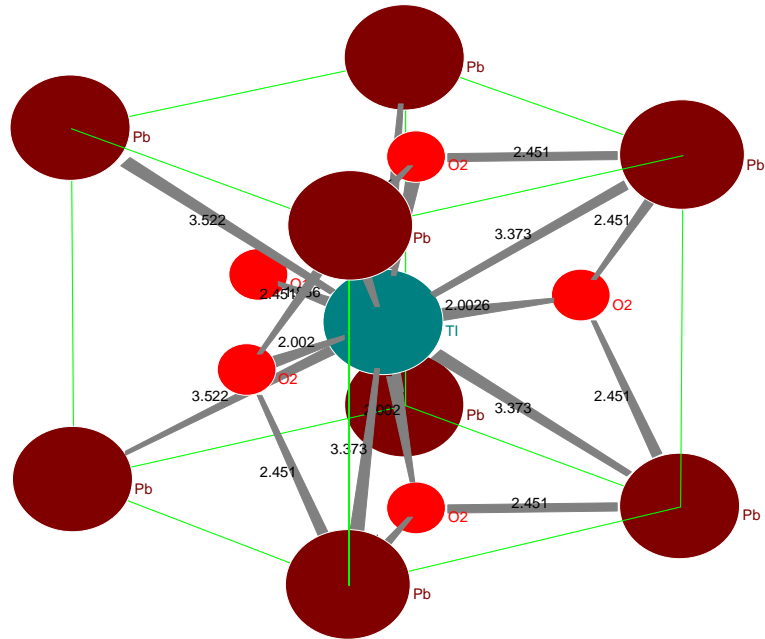
Fig.7: Structure of PbTiO$_3$ obtained from the Rietveld analysis parameters.
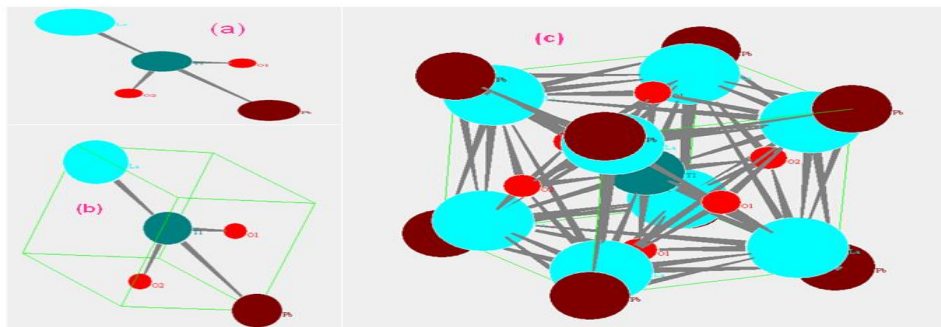

Fig.8 (a-c): (a) The position of the atom (b) the position of the atom in crystal co-ordinate and (c) the stable crystal structure of a typical sample Pb$_{0.90}$La$_{0.10}$TiO$_3$ obtained from the Rietveld analysis parameters.

4. Conclusion

PT and PLT samples prepared by solid state reaction route crystallize in a pure perovskite phase. The structure of the Pb$_{1-x}$La$_x$ TiO$_3$ ceramic samples

was examined by XRD-Rietveld refinement technique. According to XRD-Rietveld refinement, the tetragonality of the structure gradually diminishes with the increase of La content until a structural phase transition from tetragonal-to-cubic structure, which takes place in the range between 10% atom of La samples. In fact, the samples with x=0.0 crystallize in the P4mm space group, whereas the sample with ranged 10% to 50% atom of La crystallizes in the $Pm\bar{3}m$ space group. The crystallite size increases with increase of sintering temperature for both pure and substituted samples. The refinement of XRD data also confirmed the existence of only A-site vacancies, which are introduced to the stable crystal structure by the aliovalente replacement of Pb^{2+} by La^{3+} cations.

References

[1]   KK Deb, *Ferroelectrics,* **82,** 45 (1998)

[2]   PP Neves and AC Doriguetto, *J. Phys.* **Chem** B **108**, 14840 (**2004**) (39)

[3]   N Sahu, M Kar. and S Panigrahi, *J. Arch. Phys. Res*, **1,** 75(2010) (1)

[4]   N Sahu, M Kar, S.Panigrahi, *Int. J. phys.*, **3,** 157(2010) (2)

[5]   N Sahu, S Panigrahi, M Kar, *J.Adv.Powd.Tech.* **22,** 689 (2011)

[6]   N Sahu, and S Panigrahi. *Bull. Mater. Sci*. **34(7)**, 1 (2011)

[7]   N Sahu, S Panigrahi, *Ceramics International* **38**, 1085 (2012)

[8]   N. Sahu, S. Panigrahi and M.Kar*, Ceramics International* **38** (2012) 1549–1556**.**

[9]   N Sahu, and S Panigrahi, *Bulletin of Material Science*, **36**, 699 (2013)

[10] PM. Woodward, *Acta. Cryst*. B**53**, 32 (1997)

[11] K Okazaki, K Nagata. *Am Ceram Soc.* **52**, 85 (1973)

[12] MN Rahaman., "Sintering of Ceramics", CRC Press/Taylor and Francis Group, Boca   Raton, **55** (2008).

[13] M Kuwabara, K Goda, K Oshima., *Phys. ReV. B* **42**, 10012 (1990)

[14] RD Shannon, *Acta Crystallogr*. **751**, A 32 (1976)

[15] ECS Tavares, PS Pizani, JA Eiras, *Appl. Phys. Lett*. **72**, 897 (1998)

[16] G Singh,VS Tiwari, *J.Appl.Phys*.**106**, 124104 (2009)

[17] K Wójcik, *Ferroelectrics.* **99**, 5 (1989)

[18] XY Lang, Q Jiang, J Nanopart. *Res*. **9**, 595 (2007)

[19] M Kuwabara, K Goda, K Oshima., *Phys. ReV. B* **42**, 10012 (1990)

[20] G Shirane, R Pepinsky, BC Frazer., *Phys. ReV*. **97**, 1179 (1955)

[21] P Scherrer., *Math Phys K*, **1**, 98 (1918)

[22] GK Williamson, WH Hall, *Acta Met*. **1**, 22 (1953)

[23] RA Young, "*The Rietveld Method" International Union of Crystallography*, (New York, Oxford University Press 1996).